

The UV/X-ray emission of the symbiotic star AG Draconis during quiescence and the 1994/1995 outbursts[★]

J. Greiner¹, K. Bickert¹, R. Luthardt², R. Viotti³, A. Altamore⁴, R. González-Riestra^{5,★★}, and R.E. Stencel⁶

¹ Max-Planck-Institut für extraterrestrische Physik, D-85740 Garching, Germany

² Sternwarte Sonneberg, D-96515 Sonneberg, Germany

³ Istituto di Astrofisica Spaziale, CNR, Via Enrico Fermi 21, I-00044 Frascati, Italy

⁴ Dipartimento di Fisica E. Amaldi, Università Roma III, I-00146 Roma, Italy

⁵ IUE Observatory, ESA, Villafranca del Castillo, P.O. Box 50727, E-28080 Madrid, Spain

⁶ Department of Physics and Astronomy, University of Denver, Denver, CO 80208, USA

Received 7 May 1996 / Accepted 22 November 1996

Abstract. We present the results of an extensive campaign of coordinated X-ray (*ROSAT*) and UV (*IUE*) observations of the symbiotic star AG Dra during a long period of quiescence followed recently by a remarkable phase of activity characterized by two optical outbursts. The major optical outburst in June 1994 and the secondary outburst in July 1995 were covered by a number of target of opportunity observations (TOO) with both satellites. Optical photometry is used to establish the state of evolution along the outburst.

Our outburst observations are supplemented by a substantial number of X-ray observations of AG Dra during its quiescent phase between 1990–1993. Near-simultaneous *IUE* observations at the end of 1992 are used to derive the spectral energy distribution from the optical to the X-ray range. The X-ray flux remained constant over this three year quiescent phase. The hot component (i.e. X-ray emitting compact object) turns out to be very luminous: a blackbody fit to the X-ray data in quiescence with an absorbing column equal to the total galactic N_{H} in this direction gives $(9.5 \pm 1.5) \times 10^{36}$ (D/2.5 kpc)² erg/s. This suggests that the compact object is burning hydrogen-rich matter on its surface even in the quiescent (as defined optically) state at a rate of $(3.2 \pm 0.5) \times 10^{-8}$ (D/2.5 kpc)² M_{\odot} /yr. Assuming a steady state, i.e. burning at precisely the accretion supply rate, this high rate suggests a Roche lobe filling cool companion though Bondi-Hoyle accretion from the companion wind cannot be excluded.

With *ROSAT* observations we have discovered a remarkable decrease of the X-ray flux during both optical maxima, followed by a gradual recovering to the pre-outburst flux. In the UV these events were characterized by a large increase of

the emission line and continuum fluxes, comparable to the behaviour of AG Dra during the 1980–81 active phase. The anticorrelation of X-ray/UV flux and optical brightness evolution is very likely due to a temperature decrease of the hot component. Such a temperature decrease could be the result of an increased mass transfer to the burning compact object, causing it to slowly expand to about twice its original size during each optical outburst.

Key words: binaries: symbiotic – stars: individual: AG Dra – ultraviolet: stars – X-rays: stars – white dwarfs

1. Introduction

Symbiotic stars are characterized by the simultaneous occurrence in an apparently single object of two temperature regimes differing by a factor of 30 or more. The spectrum of a symbiotic star consists of a late type (M-) absorption spectrum, highly excited emission lines and a blue continuum. Generally, symbiotic stars are interpreted as interacting binary systems consisting of a cool luminous visual primary and a hot compact object (white dwarf, subdwarf) as secondary component. Because of mass loss of the giant there is often a common nebulous envelope. Mass transfer from the cool to the hot component is expected. An extensive review on the properties of symbiotic stars can be found in Kenyon (1986).

Many symbiotic stars show outburst events at optical and UV wavelengths. Though several models have been proposed to explain these outbursts, it is the combination of quiescent properties and these outburst properties which make it difficult to derive a consistent picture for some symbiotics.

The symbiotic star AG Draconis (BD +67°922) plays an outstanding role inside this group of stars because of its high

Send offprint requests to: J. Greiner (jgreiner@aip.de)

[★] Based on observations made with the *International Ultraviolet Explorer* collected at the Villafranca Satellite Tracking Station of the European Space Agency, Spain.

^{★★} Also Astronomy Division, Space Science Department, ESTEC.

galactic latitude, its large radial velocity of $v_r = -148$ km/s and its relatively early spectral type (K). AG Dra is probably a metal poor symbiotic binary in the galactic halo.

Here, we use all available *ROSAT* data to document the X-ray light curve of AG Dra over the past 5 years. In addition, we report on the results of the coordinated *ROSAT/IUE* campaign during the 1994/1995 outbursts. Preliminary results on the *IUE* and optical observations were given by Viotti et al. (1994a, 1994b). After a description of the relevant previous knowledge of the AG Dra properties in the optical, UV and X-ray range in the remaining part of this paragraph, we present our observational results in paragraph 2–4, discuss the various implications on the AG Dra system parameters in paragraph 5 and end with a summary in paragraph 6.

1.1. AG Dra: the optical picture

Like in most symbiotic stars, the historical light curve of AG Dra is characterized by a sequence of active and quiescent phases (e.g. Robinson 1969, Viotti 1993). The activity is represented by 1–2 mag light maxima (currently called *outbursts* or *eruptions*) frequently followed by one or more secondary maxima. It has been noted (Robinson 1969, Iijima et al. 1987) that the major outbursts occur in ≈ 15 yr intervals. This recurrence period has continued with the recent major outbursts of 1981 and 1994. Iijima et al. (1987) suggest that the major outbursts seem to occur at about the same orbital phase, shortly after the photometric maximum, i.e. shortly after the spectroscopic conjunction of the companion (hot component in front of the cool component). Occasionally, AG Dra also undergoes smaller amplitude outbursts, such as those in February 1985 and January 1986.

Between the active phases AG Dra is spending long periods (few years to decades) at minimum light ($V \approx 9.8$ – 10.0 , Mattei 1995), with small (0.1 mag) semiregular photometric variations in B and V with pseudo-periods of 300–400 days (Luthardt 1990). However, in the U band regular variations with amplitudes of 1 mag and a period of 554 days have been discovered by Meinunger (1979), and confirmed by later observations (e.g. Kaler 1987, Hric et al. 1994, Skopal 1994). This periodicity is associated with the orbital motion of the system, as confirmed by the radial velocity observations of Kenyon & Garcia (1986), Mikolajewska et al. (1995) and Smith et al. (1996). Because of the color dependence these U band variations certainly reflect the modulation of the Balmer continuum emission. The photometric variability is continuous, suggesting periodic eclipses of an extended hot region by the red giant.

In June 1994 Graslo et al. (1994) announced that AG Dra was starting a new active phase which was marked by a rapid brightening from $V=9.9$ to $V=8.4$ on June 14th, and to 8.1 on July 6–10, 1994. After July 1994 the brightness gradually declined reaching the quiescent level ($V \approx 9.8$) in November 1994. Like the 1981–82 and 1985–86 episodes, AG Dra underwent a secondary outburst in July 1995, reaching the light maximum of $V=8.9$ by the end of the month.

The optical spectrum of AG Dra was largely investigated especially in recent years, during both the active phases and

quiescence. The spectrum is typical of a symbiotic star, with a probably stable cool component which dominates the yellow-red region, and a largely variable “nebular” component with a strong blue-ultraviolet continuum and a rich emission line spectrum (e.g. Boyarchuk 1966). According to most authors the cool component is a K3 giant, which together with its large radial velocity (-148 km s^{-1}) and high galactic latitude ($b^{\text{II}} = +41^\circ$), would place AG Dra in the halo population at a distance of about 1.2 kpc, 0.8 kpc above the galactic plane. While Huang et al. (1994) suggested that the cool component of AG Dra may be of spectral type K0Ib, which would place it at a distance of about 10 kpc, Mikolajewska et al. (1995) from a comparison with the near-infrared colors of M3 and M13 giants concluded that the cool component is a bright giant with $M_{\text{bol}} \gtrsim -3.5$, placing AG Dra at about 2.5 kpc. Most recently, Smith et al. (1996) performed a detailed abundance analysis and found a low metallicity ($[\text{Fe}/\text{H}] = -1.3$), a temperature of $T_{\text{eff}} = 4300 \pm 100$ K and $\log g = 1.6 \pm 0.3$ consistent with the classification of AG Dra’s cool component as an early K giant. In the following we shall assume a distance of 2.5 kpc for the AG Dra system.

1.2. AG Dra: the UV picture

The hot dwarf companion is a source of intense ultraviolet radiation which produces a rich high-temperature emission line spectrum and a strong UV continuum. AG Dra is in fact a very bright UV target which has been intensively studied with *IUE* (e.g. Viotti et al. 1983, Lutz et al. 1987, Kafatos et al. 1993, Mürset et al. 1991, Mikolajewska et al. 1995).

Ultraviolet high-resolution spectra with the *IUE* satellite revealed high-ionization permitted emission lines such as the resonance doublets of Nv, Crv and Siv. The strongest emission line is HeII $\lambda 1640$ which is composed of narrow and broad (FWHM = 6 Å, or equivalently ≈ 1000 km/s) components. The Nv line has a P Cygni absorption component displaced 120 km/s from the emission peak (Viotti et al. 1983).

The origin of this feature is unclear. It can either arise in the red-giant wind ionized by the hot dwarf radiation, or in some low-velocity regions of the hot component’s wind.

The UV continuum and line flux is largely variable with the star’s activity. Viotti et al. (1984) studied the *IUE* spectra of AG Dra during the major 1980–1983 active phase, and found that the outburst was most energetic in the ultraviolet with an overall rise of about a factor 10 in the continuum, much larger than in the visual, and of a factor 2–5 in the emission line flux. A large UV variation was also a characteristic of the minor 1985 and 1986 outbursts (e.g. Mikolajewska et al. 1995).

1.3. AG Dra: the X-ray picture

First X-ray observations of AG Dra during the quiescent phase were done with the HEAO-2 satellite (*Einstein* Observatory) before the 1981–1985 series of eruptions (0.27 IPC counts/sec). The spectrum was found to be very soft (Anderson et al. 1981). The data are consistent with a blackbody source of $kT = 0.016$ keV (Kenyon 1988) in addition to the bremsstrahlung source

($kT=0.1$ keV) suggested by Anderson et al. (1981). The X-ray temperature of $\approx 200\,000$ K is in fair agreement with the source temperature of $\approx 100\,000$ – $150\,000$ K inferred from *IUE* observations, although the blackbody radius deduced from *IUE* data is nearly a factor of 10 larger than the X-ray value (Kenyon 1988). Unfortunately, the major 1980 outburst was “lost” by the HEAO-2 satellite because of a failure of the high voltage power.

A comparison of the X-ray flux with the observed HeII $\lambda 4686$ flux indicates that the luminosity in absorbed He⁺ photons is larger by a factor of two (Kenyon 1988). It has been concluded that the X-rays are degraded by the surrounding nebula thus causing an underestimate of the actual X-ray luminosity.

EXOSAT was pointed on AG Dra four times during the 1985–86 minor active phase, which was characterized by two light maxima in February 1985 and January 1986. These observations revealed a large X-ray fading with respect to quiescence (Piro 1986), the source being at least 5–6 times weaker in the *EXOSAT* thin Lexan filter in March 1985, and not detected in February 1986 (Viotti et al. 1995). Simultaneous *IUE* observations have on the contrary shown an increase of the continuum and emission line flux, especially of the high temperature Nv 1240 Å and HeII 1640 Å lines at the time of the light maxima. According to Friedjung (1988) this behaviour might be due to a temperature drop of a non-black body component, or to a continuous absorption of the X-rays shortwards of the N⁺ ionization limit. No eclipse of the X-ray source was found at phase 0.5 (beginning of November 1985) of the orbital motion of the AG Dra system, implying a limit in the orbit inclination. The weakness of the countrate in the Boron (filter #6) *EXOSAT* filter during quiescence implies a low (2 – 3×10^5 K) temperature of the source (Piro et al. 1985).

2. Optical observations

AG Dra is included in a long-term programme of optical photometry at the 60 cm Cassegrain telescope of Sonneberg Observatory. A computer controlled, photoelectric photometer with a diaphragm of 20'' diameter is used to obtain consecutive UB_V images of AG Dra, the comparison star BD+67 952 and a third star (SAO 16935) used for check purposes. Typical integration times were 20 sec and the brightnesses were reduced to the international system according to Johnson. The mean errors in the brightness determination are ± 0.01 mag in V and B and ± 0.03 mag in U. The photometric observations since June 1990 (for which near-simultaneous X-ray measurements with *ROSAT* are available) are tabulated in Table 1 and the U and B magnitudes are also plotted in Fig. 3. Earlier Sonneberg photometric data of AG Dra are included in Hric et al. (1993).

In addition to the photoelectric data we have also used the photographic sky patrol of Sonneberg Observatory to fill up gaps in the photoelectric coverage. The sky patrol is performed simultaneously in two colors (red and blue). The brightness measurements of AG Dra from the blue plates covering the time interval of the two optical outbursts are given in Table 2 and are also plotted in the top panel of Fig. 3.

Table 1. Photometric observations of AG Dra at Sonneberg Observatory (see paragraph 2 for details).

HJD	V (mag)	HJD	B (mag)	HJD	U (mag)
8127.3876	9.76	8127.3913	11.15	8127.3991	11.77
8179.3537	9.85	8179.3592	11.25		
8179.3537	9.85	8179.3613	11.26	8179.3696	11.66
8274.6330	9.83	8274.6384	11.20	8274.6432	11.37
8329.6163	9.76	8329.6212	11.10	8329.6265	11.32
8332.5781	9.76	8332.5840	11.11	8332.5908	11.34
8353.5254	9.69	8353.5317	11.06	8353.5380	11.36
8359.5031	9.70	8359.5076	11.07	8359.5135	11.31
8362.5344	9.72	8362.5425	11.07	8362.5498	11.33
8409.4444	9.73	8409.4491	11.08	8409.4544	11.28
8440.4711	9.71	8440.4755	11.09	8440.4809	11.43
8494.3874	9.77	8494.3916	11.15	8494.3978	11.67
8500.4155	9.74	8500.4208	11.11	8500.4275	11.64
8681.4692	9.71	8681.4732	11.08	8681.4785	11.54
8691.6060	9.73	8691.6099	11.08	8691.6153	11.59
8747.4630	9.72	8747.4699	11.02	8747.4767	11.33
8801.4260	9.75	8801.4301	11.08	8801.4362	11.35
8803.4410	9.74	8803.4480	11.08	8803.4540	11.33
8830.3997	9.85	8830.4040	11.19	8830.4107	11.41
8843.3743	9.83	8843.3781	11.18	8843.3831	11.31
9213.3667	9.41	9213.3746	10.40	9213.3818	9.89
9214.4254	9.48	9214.4333	10.53	9214.0000	10.42
9215.3892	9.54	9215.3981	10.62	9215.4061	10.28
9217.3517	9.49	9217.3587	10.57	9217.3648	10.15
9249.3329	9.63	9249.3385	10.83	9249.3448	10.56
9250.3517	9.64	9250.3581	10.82	9250.3639	10.54
9534.4792	8.89	9534.4863	9.56	9534.4931	8.60
9535.4286	8.77	9535.4350	9.34	9535.4419	8.43
9537.4377	8.67	9537.4436	9.22	9537.4494	8.32
9541.4588	8.46	9541.4740	8.96	9541.4790	8.04
9545.4204	8.55	9545.4266	9.02	9545.4327	8.15
9568.4060	8.61	9568.4117	9.09	9568.4182	8.30
9569.4107	8.62	9569.4172	9.11	9569.4229	8.28
9599.3582	8.85	9599.3688	9.50	9599.3760	8.72
9623.4056	9.06	9623.4124	9.78	9623.4187	9.07
9625.4310	9.07	9625.4376	9.80	9625.4438	9.09
9638.3671	9.17	9638.3732	9.92	9638.3791	9.19
9639.3749	9.15	9639.3824	9.96	9639.3885	9.25
9644.4397	9.19	9644.4462	9.97	9644.4544	9.20

3. IUE observations

IUE observations were mostly obtained as a Target-of-Opportunity (TOO) programme in coordination with the *ROSAT* observations. The last observations were made within the approved programme SI047 for the 19th *IUE* observing episode. Table 3 summarizes the *IUE* low resolution observations made in the period June 1994 – September 1995.

In general, priority was given to the low resolution spectra for line and continuum fluxes. High resolution spectra were also taken at all dates, but they will not be discussed in this paper. For most of the low resolution images, both *IUE* apertures were used in order to have in the Large Aperture the continuum and the emission lines well exposed and in the Small Aperture (not pho-

Table 2. Photographic observations of AG Dra at Sonneberg Observatory (see paragraph 2 for details).

HJD	m_{pg} (mag)	HJD	m_{pg} (mag)
9002.317	10.6	9476.471	10.6
9005.310	10.6	9476.491	10.5
9027.258	10.6	9476.491	10.4
9028.259	10.5	9480.480	10.6
9029.263	10.7	9480.480	10.5
9030.298	10.7	9480.480	10.5
9031.303	10.5	9481.488	10.5
9032.300	10.8	9481.488	10.4
9041.276	10.8	9481.488	10.6
9066.531	11.0	9482.487	10.5
9094.472	11.0	9482.487	10.5
9094.472	10.5	9482.487	10.4
9098.500	11.0	9484.494	10.4
9098.500	10.7	9484.494	10.4
9099.486	11.0	9484.494	10.5
9099.486	10.9	9486.456	10.5
9101.507	11.0	9486.456	10.3
9101.507	10.9	9486.456	10.4
9154.458	11.0	9488.493	10.5
9154.458	10.9	9488.493	10.5
9249.496	10.8	9488.493	10.5
9250.487	10.6	9504.419	9.4
9278.519	10.5	9511.453	9.2
9279.468	10.5	9518.458	9.1
9310.486	10.7	9535.417	9.0
9416.304	10.5	9536.422	9.0
9422.549	10.7	9537.423	8.9
9422.549	10.7	9541.415	8.9
9422.549	10.6	9574.422	8.7
9457.489	10.5	9836.477	10.0
9457.499	10.5	9839.479	10.0
9457.499	10.5	9840.483	10.2
9458.517	10.5	9841.511	10.3
9458.517	10.4	9842.522	10.1
9458.517	10.6	9862.443	10.1
9462.550	10.5	9888.422	10.3
9462.550	10.4	9889.422	10.0
9462.550	10.6	9894.422	9.9
9475.478	10.5	9895.422	9.8
9475.478	10.4	9896.417	9.9
9475.478	10.6		

tometric) the strongest emission lines (essentially HeII 1640 Å) not saturated. The fluxes from the Small Aperture spectra were corrected for the smaller aperture transmission by comparison with the non-saturated parts of the Large Aperture data. Some representative IUE spectra are shown in Fig. 1.

The flux of the strongest emission lines and of the continuum flux at 1340 and 2860 Å is given in Table 4. All the fluxes are corrected for an interstellar absorption of $E(B-V)=0.06$ (Viotti et al. 1983). The feature at 1400 Å is a blend, unresolved at low resolution of the SiIV doublet at 1393.73 and 1402.73 Å, the OrV] multiplet (1399.77, 1401.16, 1404.81 and 1407.39 Å), and SrV] 1402.73 Å. OrV] 1401.16 Å is the dominant contributor

Table 3. Journal of AG Dra low resolution IUE observations

Image ^a	Disp	Aper ^b	Date dd/mm/yy	T _{exp} ^c min:sec
SWP51315	L	L,S	04/07/94	15:00,5:00
LWP28542	L	L,S	04/07/94	7:00,3:00
SWP51331	L	L,S	07/07/94	2:00,2:00
LWP28556	L	L,S	07/07/94	1:30,1:00
SWP51415	L	L,S	12/07/94	1:00,1:00
LWP28628	L	L,S	12/07/94	1:00,1:00
SWP51416	L	L,S	12/07/94	1:35,1:35
SWP51632	L	L,S	28/07/94	2:00,1:00
LWP28752	L	L,S	28/07/94	2:00,1:00
SWP52143	L	L	19/09/94	1:30
LWP29192	L	L	19/09/94	1:00
SWP52145	L	L	19/09/94	3:00
SWP52994	L	L,S	06/12/94	3:00,2:00
LWP29654	L	L,S	06/12/94	2:00,2:00
SWP54632	L	L,S	08/05/95	3:00,1:30
LWP30642	L	L,S	08/05/95	2:00,1:00
SWP55371	L	L,S	28/07/95	1:00,1:00
LWP31175	L	L,S	28/07/95	2:00,1:00
SWP55929	L	L,S	14/09/95	2:00,1:00
LWP31476	L	L,S	14/09/95	3:00,1:30

^a SWP: 1200-1950 Å. LWP: 1950-3200 Å.

^b L, S: both large and small IUE apertures were used. L: only the large aperture was used.

^c Two exposure times correspond to Large and Small aperture, respectively.

to the blend. Because of the variable intensity of the lines, at low resolution the 1400 Å feature shows extended wings with variable extension and strength (Fig. 1). The two continuum regions were chosen, as in previous works, for being less affected by the emission lines, and for being the 1340 Å representative of the continuum of the hot source (nearly the Rayleigh-Jeans tail of a 10^5 K blackbody), and the 2860 Å region representative of the HII Balmer continuum emission (see for instance Fernández-Castro et al. 1995).

The behaviour of the continuum and line intensities is shown in Fig. 2. In July 1994 the UV continuum flux increase was larger than that of the HeII 1640 Å line, suggesting a decrease of the Zanstra temperature at the time of the outburst, and a recovering of the high temperature in September 1994. In addition, the NV/continuum (1340 Å) and the HeII/continuum (1340 Å) ratios reached a maximum at the time of the second outburst (July 1995). The HeII Zanstra temperatures are given in Fig. 3.

4. ROSAT observations

4.1. Observational details

4.1.1. All-Sky-Survey

AG Dra was scanned during the All-Sky-Survey over a time span of 10 days. The total observation time resulting from 95 individual scans adds up to 2.0 ksec. All the ROSAT data anal-

Table 4. Ultraviolet fluxes^a of AG Dra in outburst. Typical quiescent fluxes are given in the first line (Viotti et al. 1984, Meier et al. 1994).

Date ^b	NV	1400 ^c	CIV	HeII	F ₁₃₄₀	F ₂₈₆₀
quiescence	10	8	9	26	29	12
9537	52	32	114	237	607	368
9538	41	26	99	277	535	367
9545	35	25	80	221	656	407
9560	19	17	49	197	526	303
9612	39	23	50	150	299	191
9692	23	11	32	121	166	83
9844	29	11	25	195	144	64
9926	36	61 ^d	59	183	137	158
9975	36	31	68	172	155	55

^a Emission line (in 10^{-12} erg cm⁻² s⁻¹) and continuum fluxes (in 10^{-14} erg cm⁻² s⁻¹ Å⁻¹), dereddened for $E_{B-V}=0.06$.

^b JD - 2440000.

^c Blend of O IV] and Si IV. O IV] $\lambda 1401.16$ is the main contributor to the blend.

^d Broad feature.

ysis described in the following has been performed using the dedicated EXSAS package (Zimmermann et al. 1994).

Due to the scanning mode the source has been observed at all possible off-axis angles with its different widths of the point spread function. For the temporal and spectral analysis we have used an 5' extraction radius to ensure that no source photons are missed. No other source down to the 1σ level is within this area. Each photon event has been corrected for its corresponding effective area. The background was determined from an equivalent area of sky located circle 13' south in ecliptic latitude from AG Dra.

4.1.2. Pointed observations

Several dedicated pointings on AG Dra have been performed in 1992 and 1993 with the ROSAT PSPC (Table 5 gives a complete log of the observations). All pointings were performed with the target on-axis. During the last ROSAT observation of AG Dra with the PSPC in the focal plane (already as a TOO) the Boron filter was erroneously left in front of the PSPC after a scheduled calibration observation.

For each pointed observation with the PSPC in the focal plane, X-ray photons have been extracted within 3' of the centroid position. This relatively large size of the extraction circle was chosen because the very soft photons (below channel 20) have a much larger spread in their measured detector coordinates. As usual, the background was determined from a ring well outside the source (there are no other X-ray sources within 5' of AG Dra). Before subtraction, the background photons were normalized to the same area as the source extraction area.

When AG Dra was reported to go into outburst (Granslo et al. 1994) we immediately proposed for a target of opportunity observation (TOO) with ROSAT. AG Dra was scheduled to be observed during the last week of regular PSPC observations on July 7, 1994, but due to star tracker problems no photons were collected. For all the later ROSAT observations only the HRI

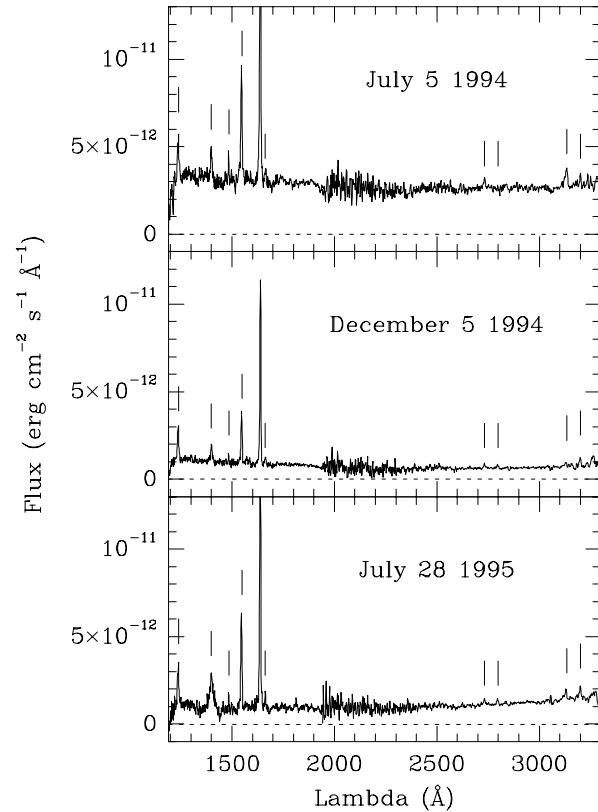


Fig. 1. IUE spectra of AG Dra at three different dates during the 1994-1995 activity phase: during the 1994 outburst (top), during the “quiescent” state between the outbursts (middle) and during the second outburst (bottom). The strongest line in the three spectra is HeII 1640 Å. The lines marked in the spectra are: NV 1240 Å, the blend SiIV + OIV] 1400 Å, NIV] 1486 Å, CIV 1550 Å, OIII] 1663 Å, HeII 2733 Å, MgII 2800 Å, OIII 3133 Å and HeII 3202 Å.

could be used after the PSPC gas has been almost completely exhausted. Consequently, no spectral information is available for these observations. The first HRI observation took place on August 28, 1994, about 4 weeks after the optical maximum. All the following HRI observations and the single PSPC observation with the Boron filter (described above) were performed as TOO to determine the evolution of the X-ray emission after the first outburst. With the knowledge of the results of the first outburst the frequency of observations was increased for the second optical outburst.

Source photons of the HRI observations have been extracted within 1' and were background and vignetting corrected in the standard manner using EXSAS tasks. In order to compare the HRI intensities of AG Dra with those measured with the PSPC we use a PSPC/HRI countrate ratio for AG Dra with its supersoft X-ray spectrum of 7.8 as described in Greiner et al. (1996).

4.2. The X-ray position of AG Dra

We derive a best-fit X-ray position from the on-axis HRI pointing 180073 of R.A. (2000.0) = 16^h01^m40^s.8, Decl. (2000.0) = 66°48'08" with an error of $\pm 8''$. This position is only 2" off

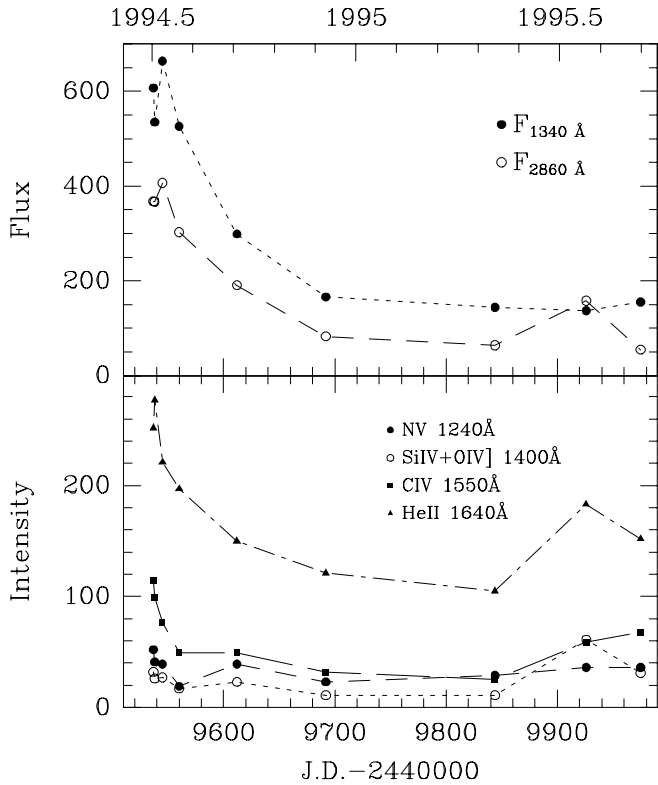


Fig. 2. Evolution of the UV continuum and emission lines of AG Dra during the 1994-1995 outburst. Units of continuum fluxes are 10^{-14} erg $\text{cm}^{-2} \text{s}^{-1} \text{\AA}^{-1}$, and of line intensities 10^{-12} erg $\text{cm}^{-2} \text{s}^{-1}$. All the measurements are corrected for an interstellar reddening of $E(B-V)=0.06$.

the optical position of AG Dra (R.A. (2000.0) = $16^{\text{h}}01^{\text{m}}40^{\text{s}}.94$, Decl. (2000.0) = $66^{\circ}48'09''.7$).

4.3. The X-ray lightcurve of AG Dra

The mean ROSAT PSPC countrate of AG Dra during the all-sky survey was determined (as described in paragraph 4.1.1) to (0.99 ± 0.15) cts/sec. Similar countrates were detected in several PSPC pointings during the quiescent time interval 1991–1993.

The X-ray light curve of AG Dra as deduced from the All-Sky-Survey data taken in 1990, and 11 ROSAT PSPC pointings (mean countrate over each pointing) as well as 7 HRI pointings taken between 1991 and 1996 is shown in Fig. 3. The countrates of the HRI pointings have been converted with a factor of 7.8 (see paragraph 4.1.2) and are also included in Fig. 3.

This 5 yrs X-ray light curve displays several features:

1. The X-ray intensity has been more or less constant between 1990 and the last observation (May 1993) before the optical outburst. Using the mean best fit blackbody model with $kT = 14.5$ eV and the galactic column density $N_{\text{H}} = 3.15 \times 10^{20} \text{ cm}^{-2}$ (fixed during the fit, see below), the unabsorbed intensity in the ROSAT band (0.1–2.4 keV) is $1.2 \times 10^{-9} \text{ erg cm}^{-2} \text{ s}^{-1}$.
2. During the times of the optical outbursts the observed X-ray flux drops substantially. The observed maximum amplitude

Table 5. Summary of ROSAT observations on AG Dra. Given are for each pointing the observation ID (column 1), the date of the observation (2), the detector (P=PSPC, H=HRI) without or with Boron (B) filter (3), the nominal exposure time (4), and the total number of counts (5).

ROR No.	Date	P/H	T_{Nom} (sec)	N_{cts}
Survey	Nov. 24–Dec. 3, 1990	P	2004	1988
200686	April 16, 1992	P	2178	2260
200687	May 16, 1992	P	1836	1761
200688	June 13, 1992	P	2210	2224
201041	June 16, 1992	P	1829	1893
201042	Sep. 20, 1992	P	1596	1676
201043	Dec. 16, 1992	P	1296	1344
200689	March 13, 1993	P	1992	2029
201044	March 16, 1993	P	1677	1761
200690	April 15, 1993	P	2450	2324
200691	May 12, 1993	P	2064	1669
180063	Aug. 28, 1994	H	1273	14
180063F	Sep. 9, 1994	P(B)	1237	19
180073	Dec. 7, 1994	H	2884	209
180073-1	Mar. 7, 1995	H	2330	272
180081	Jul. 31, 1995	H	1191	22
180081-1	Aug. 23, 1995	H	916	5
180081-2	Sep. 14, 1995	H	1383	0
180081-3	Feb. 6, 1996	H	1551	88

of the intensity decrease is nearly a factor of 100. With the lowest intensity measurement being an upper limit, the true amplitude is certainly even larger. Due to the poor sampling we cannot determine whether the amplitudes of the two observed X-ray intensity drops are similar.

3. Between the two X-ray minima the X-ray intensity nearly reached the pre-outburst level, i.e. the relaxation of whatever parameter caused these drops was nearly complete. We should, however, note that the relaxation to the pre-outburst level was faster at optical wavelength than at X-rays, and also was faster in the B band than in the U band. In December 1994 the optical V brightness ($\approx 9^{\text{m}}.5$) was nearly back to the pre-outburst magnitude, while the X-ray intensity was still a factor of 2 lower than before the outburst.
4. The quiescent X-ray light curve shows two small, but significant intensity drops in May 1992 and April/May 1993. The latter and deeper dip coincides with the orbital minimum in the U lightcurve (Meinunger 1979, Skopal 1994) and might suggest a periodic, orbital flux variation.

4.4. The X-ray spectrum of AG Dra in quiescence

For spectral fitting of the all-sky-survey data the photons in the amplitude channels 11–240 (though there are almost no photons above channel 50) were binned with a constant signal/noise ratio of 9σ . The fit of a blackbody model with all parameters left free results in an effective temperature of $kT_{\text{bb}} = 11$ eV (see Table 6).

Since the number of counts detected during the individual PSPC pointings allows high signal-to-noise spectra, we investi-

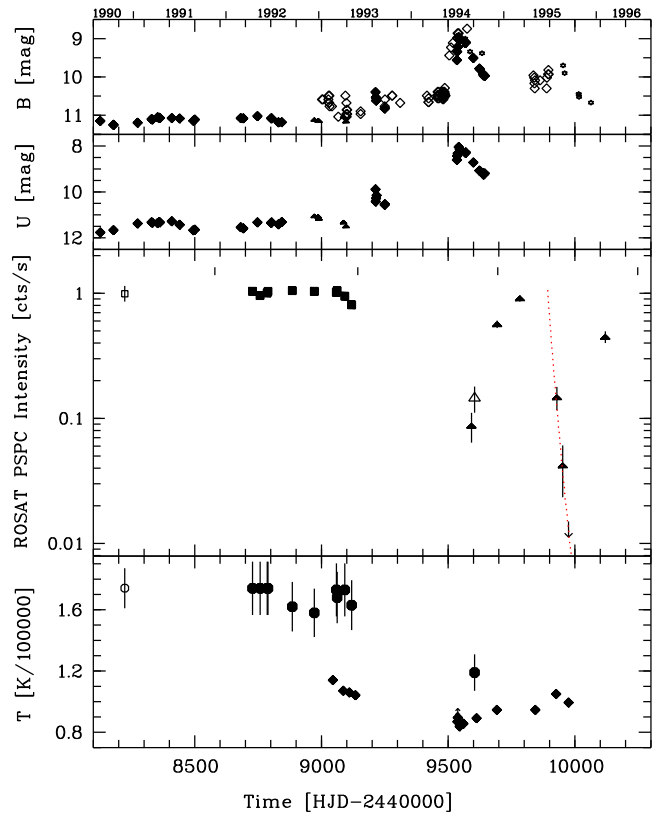


Fig. 3. The X-ray and optical light curve of AG Dra over the past 5 years. The two top panels show the U and B band variations as observed at Sonneberg Observatory (filled lozenges = photoelectric photometry, open lozenges = photographic sky patrol), Skalnaté Pleso Observatory (Hric et al. 1994; filled triangles), and Italian amateurs (Montagnani et al. 1996; stars). The large middle panel shows the X-ray intensity as measured with the *ROSAT* satellite: filled squares denote PSPC observations, filled triangles are HRI observations with the countrate transformed to PSPC rates (see text), and the open triangle is the Boron filter observation corrected for the filter transmission. Statistical errors (1σ) are overplotted; those of the PSPC pointings are smaller than the symbol size. The vertical bars at the top indicate the minima of the U band lightcurve (Skopal 1994). The dotted line shows the fit of an expanding and cooling envelope to the X-ray decay light curve. The lower panel shows temperature estimates from blackbody fits to the *ROSAT* X-ray data (filled circles) and from the HeII ($\lambda 1640$) flux to continuum flux at $\lambda 1340$ Å as determined from the IUE spectra and assuming $E(B-V)=0.06$ (=Zanstra temperatures, filled lozenges).

gated the possibility of X-ray spectral changes with time. First, we kept the absorbing column fixed at its galactic value and determined the temperature being the only fit parameter. We find no systematic trend of a temperature decrease (lower panel of Fig. 3). Second, we kept the temperature fixed (at 15 eV in the first run and at the best fit value of the two parameter fit in the second run) and checked for changes in N_H , again finding no correlation. Thus, no variations of the X-ray spectrum could be found along the orbit. The rather small degree of observed variation of temperature and N_H (Table 6) over more than three years during quiescence (including the *ROSAT* All-

Table 6. Summary of blackbody model fits to the *ROSAT* PSPC observations of AG Dra during quiescence. Fluxes are in photons/cm²/s and temperatures kT in eV. The absorbing column N_H is in units of 10^{20} cm⁻² for the three parameter fit and was fixed at the galactic value of 3.15×10^{20} cm⁻² for the two parameter fit.

ROR No.	Date	3-parameter fit		2-parameter fit		
		N_H	Flux	kT	Flux	kT
Survey	901129	5.0	7040	10.6	172.5	14.6
200686	920416	5.1	4680	11.0	144.2	15.0
200687	920516	4.6	1280	11.7	147.0	15.0
200688	920613	4.9	2750	11.2	145.0	15.0
201041	920616	4.7	1520	11.6	146.7	15.0
201042	920920	3.5	860	13.2	304.1	14.0
201043	921216	4.2	1360	11.3	421.1	13.6
200689	930313	5.2	9060	10.6	160.1	14.9
201044	930316	4.5	1240	11.6	205.8	14.5
200690	930415	5.3	9760	10.6	147.7	14.9
200691	930512	5.1	9750	10.4	227.9	14.1

Sky-Survey data) are not regarded to be significant due to the correlation of these quantities (Fig. 4).

The independent estimate of the absorbing column towards AG Dra from the X-ray spectral fitting indicates that the detected AG Dra emission experiences the full galactic absorption. While fits with N_H as free parameter (see Table 6) systematically give values slightly higher than the galactic value (which might lead to speculations of intrinsic absorption), we assess the difference to be not significant due to the strong interrelation of the fit parameters (see lower right panel of Fig. 4) given the energy resolution of the PSPC and the softness of the X-ray spectrum. We will therefore use the galactic N_H value (3.15×10^{20} cm⁻² according to Dickey and Lockman 1990) in the following discussion.

With N_H fixed at its galactic value the mean temperature during quiescence is about 14–15 eV, corresponding to 160000–175000 K. These best fit temperatures are plotted in a separate panel below the X-ray intensity (Fig. 3). The small variations in temperature during the quiescent phase are consistent with a constant temperature of the hot component of AG Dra.

4.5. The X-ray spectrum of AG Dra in outburst

As noted already earlier (e.g. Friedjung 1988), the observed fading of the X-ray emission during the optical outbursts of AG Dra can be caused either by a temperature decrease of the hot component or an increased absorbing layer between the X-ray source and the observer. In order to evaluate the effect of these possibilities, we have performed model calculations using the response of the *ROSAT* HRI. In a first step, we assume a 15 eV blackbody model and determine the increase of the absorbing column density necessary to reduce the *ROSAT* HRI countrate by a factor of hundred. The result is a factor of three increase. In a second step we start from the two parameter best fit and determine the temperature decrease which is necessary to reduce the *ROSAT* HRI countrate at a constant absorbing column (3.15×10^{20} cm⁻²). We find that the temperature of the hot

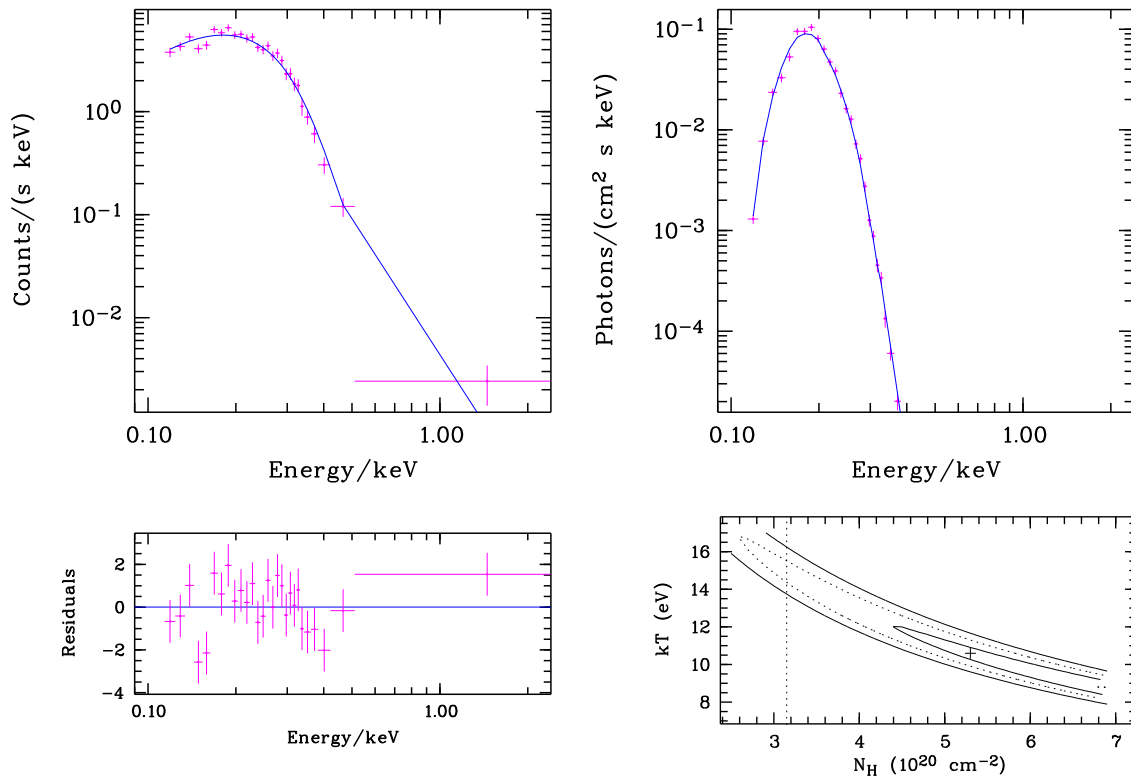


Fig. 4. ROSAT X-ray spectrum of AG Dra in quiescence on April 15, 1993. A blackbody model is used; for best fit parameters see Table 6. The upper left panel shows the countrate spectrum, while the upper right panel shows the absorbed photon spectrum after folding with the detector response. The lower left panel shows the residuals of the fit in units of σ , while the lower right panel visualizes the range of 1, 2 and 3 σ contours of the absorbing column and the best fit blackbody temperature in the three parameter fit. The cross marks the best fit and the dotted line marks the total galactic column density.

component has to decrease from 15 to 10 eV, or correspondingly from 175000 K to 115000 K.

The only ROSAT PSPC observation (i.e. with spectral resolution) during optical outburst is the one with Boron filter. The three parameter fit as well as the two parameter fit give a consistently lower temperature. But since the Boron filter cuts away the high-end of the Wien tail of the blackbody, and we have only 19 photons to apply our model to, we do not regard this single measurement as evidence for a temperature decrease during the optical outburst.

What seems to be excluded, however, is any enhanced absorbing column during the Boron filter observation. The best fit absorbing column of the three parameter fit is $4.4 \times 10^{20} \text{ cm}^{-2}$, consistent with the best fit absorbing column during quiescence. Since the low energy part of the spectrum in the PSPC is not affected by the Boron filter except a general reduction in efficiency by roughly a factor of 5, any increase of the absorbing column would still be easily detectable. For instance, an increase of the absorbing column by a factor of two (to $6.3 \times 10^{20} \text{ cm}^{-2}$) would absorb all photons below 0.2 keV and would drop the countrate by a factor of 50 contrary to what is observed.

It is interesting to note that the decrease of the X-ray flux is similarly strong in both, the 1994 and 1995 outbursts, while the optical amplitude of the secondary outburst in 1995 was

considerably smaller than the first outburst. We note in passing that the intensity of the HeII and Nv lines also showed a comparable large increase in the main 1981/1982 outburst and the minor outburst in 1985/1986 while the optical and the short wavelength UV continuum amplitudes again were smaller in the latter outburst (Mikolajewska et al. 1995). Since the short wavelength UV continuum is the Rayleigh-Jeans tail of the hot (blackbody) component, this behaviour suggests that a temperature decrease is the cause of the reduced X-ray intensity during outburst rather than increased absorption with the temperature decrease being smaller in the secondary outbursts.

5. Discussion

5.1. Quiescent X-ray emission

5.1.1. The X-ray spectrum and luminosity

Previous analyses of X-ray emission of symbiotic stars have been interpreted either with blackbody (Kenyon and Webbink 1984) or NLTE atmosphere (Jordan et al. 1994) models representing the hot component, or with bremsstrahlung emission from a hot, gaseous nebula (Kwok and Leahy 1984). Our ROSAT PSPC spectra of AG Dra show no hint for any hard X-ray emission. The soft spectrum is well fitted with a blackbody

model. A thermal bremsstrahlung fit is not acceptable to this soft energy distribution. There is also no need for a second component as proposed by Anderson et al. (1981): a fit of a blackbody and thermal bremsstrahlung model with the bremsstrahlung temperature limited to values above 0.1 keV results in an unabsorbed flux ratio between blackbody and bremsstrahlung of 85000:1 in the 0.1–2.4 keV band. A hard X-ray component could be expected from an accretion disk both for radial and disk accretion (Livio 1988) at the relatively low accretion rate implied for this system. This absence of any hard emission also rules out the possibility of interpreting the soft spectrum as arising in the boundary layer. The most extreme ratios for soft to hard emission observed so far in magnetic cataclysmic variables are of the order of 1000:1. An example of the blackbody fit is given in Fig. 4 using the observation of April 1993 (having the largest number of photons).

The simple model of explaining the soft X-ray emission by an accretion disk is ruled out not only due to the soft spectrum, but also due to the observed luminosity which is much higher (see below) than can be produced by an accretion disk around a compact dwarf and the extremely low accretion rate. If the X-ray spectrum were to be explained by a standard accretion disk model (Shakura & Sunyaev 1973) then the necessary accretion rate would be of the order of $1.7 \times 10^{-7} \dot{M}_{\text{edd}}$ (or $4.5 \times 10^{-15} M_{\odot}/\text{yr}$) for a $1 M_{\odot}$ compact object. This is unreasonably small, basically due to the low effective temperature ($T_{\text{max}}^{\text{eff}} = 24 \text{ eV}$) of the X-ray emission coupled with a small mass compact object.

Using the blackbody fit parameters while N_{H} was fixed at its galactic value, i.e. $kT = 14.5 \text{ eV}$ and a normalization parameter of 206 photons/cm²/s corresponding to observation 201044 (from experience with soft ROSAT spectra we know that this procedure helps to avoid overpredicting the flux using blackbody models), the unabsorbed bolometric luminosity of the hot component in AG Dra during quiescence (1990–1993) is $(9.5 \pm 1.5) \times 10^{36} (D/2.5 \text{ kpc})^2 \text{ erg/s}$ (or equivalently $2500 \pm 400 (D/2.5 \text{ kpc})^2 L_{\odot}$) with an uncertainty of a factor of a few due to the errors in the absorbing column and the temperature (see Fig. 5 for a visualization of the fact that the ROSAT measurement actually covers only the tail of the spectral energy distribution). The blackbody radius is derived to be $R_{\text{bb}} = (4.1 \pm 1.5) \times 10^9 \text{ cm}$ ($D/2.5 \text{ kpc}$). (Previous estimates arrived at much lower values due to the overestimate of the temperature.)

This high luminosity during quiescence and the size of the emitting region comparable to a white dwarf radius suggests that the primary is a white dwarf in the state of surface hydrogen burning. Assuming that the bolometric luminosity of the hot component equals the nuclear burning luminosity, the burning rate is $\dot{M} \approx (3.2 \pm 0.5) \times 10^{-8} (D/2.5 \text{ kpc})^2 M_{\odot}/\text{yr}$. Under the assumption of a steady state the same amount of matter should be accreted onto the white dwarf from the companion (via wind or an accretion disk, see below). Indeed, this burning rate lies within the stable-burning regime for a white dwarf of less than $0.6 M_{\odot}$ (Iben and Tutukov 1989) consistent with the core mass-luminosity relation $L/L_{\odot} \approx 4.6 \times 10^4 (M_{\text{core}}/M_{\odot} - 0.26)$ (Yungelson et al. 1996). From the orbital parameters (Mikolajewska et al. 1995, Smith et al. 1996) and an inclination less than about

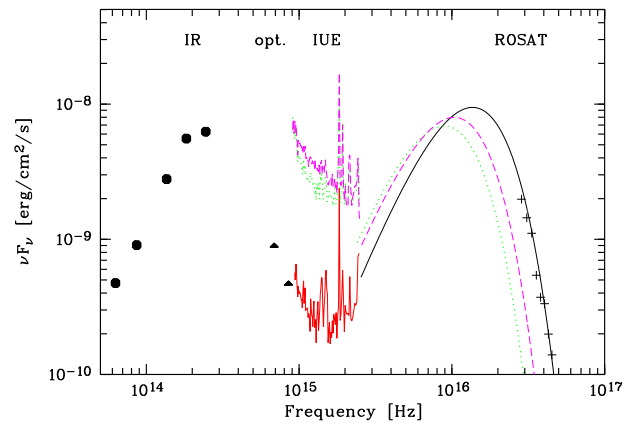


Fig. 5. Energy distribution of AG Dra during quiescence and outburst: The full line shows the quiescent spectrum, combined from a UV spectrum of April 9, 1993, and a ROSAT observation of April 15, 1993 (best fit blackbody extrapolation is shown on top of the absorption corrected data points). The optical B measurement is also from April 15, while the U measurement is from April 10, 1993. The dashed/dotted lines are the measured UV spectra during outburst of July 28 / Sep 14, 1995 together with the modelled blackbody spectra of lower temperature (11/9.5 eV) which reproduce the observed HRI countrates as measured with ROSAT on July 31 / Sep. 14, 1995.

85° (see paragraph 5.1.2) the donor mass is estimated to be lower than $2 M_{\odot}$, in agreement with the estimated surface gravity of Smith et al. (1996).

5.1.2. Orbital flux modulation?

The observational coverage of AG Dra over 1992/1993 is extensive enough to also investigate possible temporal and spectral changes of the X-ray flux along the orbital phase. Using the ephemeris from Skopal (1994) the minimum phases of AG Dra occurred in November 1991 and June 1993.

The coincidence of the U minimum and the drop in X-ray flux in mid-1993 is surprising, suggesting the possible discovery of orbital modulation of the X-ray flux. Unfortunately, we have no full coverage of the orbital period, and thus the duration of the flux depression cannot be determined. But even with the available data this duration is a matter of concern: The X-ray intensity decrease occurs very slowly over a time interval of two months, suggesting a total duration of at least 4 months if this modulation is symmetric in shape.

The radial velocity data demonstrate that during the U minima the cool companion lies in front of the hot component (cf. Mikolajewska et al. 1995). Depending on the luminosity class, the maximum duration for an eclipse of the WD by the giant (bright giant) companion is 10 (24) days, i.e. much shorter than the observed time scale at X-rays. Thus, the drop in X-ray intensity cannot be due to a WD eclipse. As evidenced by near-simultaneous IUE spectra between April and June 1993, the far-UV continuum associated to the tail of the hot component's continuum emission is not occulted, supporting the previous argument. A similar conclusion was reached when considering

the nearly complete lack of orbital variations of the short wavelength UV continuum (Mikolajewska et al. 1995). By inverting the arguments, the lack of an X-ray eclipse implies that the inclination should be less than 87° (82°) for a giant (bright giant) with $20 R_\odot$ ($70 R_\odot$) radius.

Even in the reflection model of Formigini & Leibowitz (1990), in which the eclipse of the hot component is short and its depth is expected to be considerably larger in the UV (and possibly in the soft X-ray band) than in the optical, it is difficult to imagine that a possible UV eclipse has been gone undetected.

Alternatively to an eclipse interpretation of the X-ray intensity drop just before the 1993 U band minimum, one could think of a pre-outburst which was missed in the optical region except for the marginal flux increase in the B band after JD = 244 9000. In this case the interpretation would be similar to that of the major X-ray intensity drops during the optical outbursts in 1994 and 1995 mass loss (see below). Independent of the actual behaviour around JD = 9100 it is interesting to note that there is a secure detection of a 2 mag U brightness jump coincident with a nearly 1 mag B brightness increase shortly after JD = 9200. A slight brightening by about 0.2–0.3 mag is also present in the AAVSO light curve around JD 9205–9215 (Mattei 1995).

5.1.3. Wind mass loss of the donor and accretion

Accepting the high luminosity during quiescence and consequently assuming that the hot component in the AG Dra system is in (or near to) the surface hydrogen burning regime, the companion has to supply the matter at the high rate of consumption by the hot component.

It is generally assumed (and supported by three-dimensional gas dynamical calculations of the accretion from an inhomogeneous medium) that the compact objects in symbiotic systems accrete matter from the wind of the companion according to the classical Bondi-Hoyle formula. The wind mass loss rate of the companion depends on several parameters. One of the important ones is the luminosity which governs the location with respect to the Linsky and Haisch dividing line. Accordingly, a bright giant (luminosity class II) is expected to have a considerably larger mass loss rate than a giant (luminosity class III).

As mentioned already earlier, the spectral classification and the luminosity class of the companion in the AG Dra binary system is not yet securely determined. According to the formula of Reimers (1975):

$$-\dot{M} = 4 \times 10^{-13} \eta \frac{RL}{M} M_\odot/\text{yr}$$

where R , L and M are the radius, luminosity and mass of the star in solar units, and η a constant between 0.1 and 1, depending primarily on the initial stellar mass, the commonly used K3III classification would imply a mass loss rate of $(0.2\text{--}7) \times 10^{-10} M_\odot/\text{yr}$, i.e. a factor of 100 lower than the rate necessary for steady state burning.

However, there are two additional observational hints which might help resolve the discrepancy between the expected mass loss of the cool donor and the necessary rate for a steady state

burning white dwarf: (1) The cool component of AG Dra might be brighter than an average solar-metallicity giant. A comparison of the luminosity functions of K giants with $4000 \lesssim T_{\text{eff}} \lesssim 4400$ in a low-metallicity versus solar-metallicity population has shown convincingly that low-metallicity K giants are nearly 2 mag brighter than the solar-metallicity giants (Smith et al. 1996). (2) Low-metallicity giants might have larger mass-loss rates than usual giants. From observed larger $12\mu\text{m}$ excess in symbiotics as compared to that in normal giants a larger mass loss of giants in symbiotics has been deduced (Kenyon 1988). The recent comparison of IR excesses of d-type symbiotics with that of CH and barium stars supports this evidence (Smith et al. 1996). Both of these observational hints argue for a mass loss of the cool component in AG Dra which is higher than the value derived from Reimer's formula. At present it seems premature, however, to conclude that the wind mass loss of the donor in AG Dra is large enough to supply the matter for a steady state surface burning on the white dwarf.

An additional problem with spherical accretion at very high rates is the earlier recognized fact (Nussbaumer & Vogel 1987) that the density of matter in the vicinity of the accretor is $n_{\text{H}} \approx 2 \times 10^7 (\dot{M}/10^{-7} M_\odot/\text{yr}) (V/10 \text{ km/s})^3 (M_{\text{WD}}/M_\odot)^{-2} \text{ cm}^{-3}$ (Yungelson et al. 1996), i.e. the soft X-rays of the burning accretor will be heavily absorbed.

Alternatively, one might consider the possibility that the donor overfills its Roche lobe and that the matter supply to the white dwarf occurs via an accretion disk. Several issues have to be considered: (1) Roche-lobe filling: In order to fill its Roche lobe, the donor has to be either rather massive (as compared to a usual K giant) or rather luminous. However, a donor mass larger than $\approx 2 M_\odot$ seems difficult due to the high galactic latitude and proper motion as well as on evolutionary grounds. Similarly, a binary system with a bright giant implies a larger distance as compared to a giant companion. (2) Evidence for the existence of an accretion disk: Indeed, Garcia (1986) has raised the suspicion that AG Dra contains an accretion disk. Circumstantial evidence for this comes from predictions of Roche lobe overflow, rapid flickering on timescales of the order of minutes in the optical band and the observation of double-peaked Balmer emission lines. Robinson et al. (1994) have investigated in detail the double-peaked line profile of the Balmer lines in several symbiotic stars. In the case of AG Dra they find double-peaked emission lines only in one out of three observations which were three and one year apart, respectively. Using an inclination of $i=32^\circ$ as proposed by Garcia (1986) the double-peaked profile gives an acceptable fit for an accretion disk with an inner radius of $1.1 \times 10^8 \text{ cm}$ and an outer radius of $1.3 \times 10^{10} \text{ cm}$ though the asymmetry may be explained also by self-absorption (Tomov & Tomova 1997). Recent high-resolution spectroscopy of AG Dra in the red wavelength region using AURELIE at OHP performed in December 1990 and January 1995 (i.e. during very different phases in the AG Dra orbit) revealed only a single peaked $H\alpha$ profile (Rossi et al. 1996) and Dobrzycka et al. (1996) failed to find evidence for flickering. Both of these new observational results argue against a steady accretion disk in the AG Dra system.

5.2. Quiescent UV emission

UV observations show that the hot components of symbiotic stars are located in the same quarters of the Hertzsprung-Russell diagram as the central stars of planetary nebula (Mürset et al. 1991). Due to the large binary separation in symbiotic systems the present hot component (or evolved component) should have evolved nearly undisturbed through the red giant phase. However, the outermost layers of the white dwarf might be enriched in hydrogen rich material accreted from the cool companion.

Presently the far-UV radiation of the WD is ionizing a circumstellar nebula, mostly formed (or filled in) by the cool star wind. The UV spectroscopy suggests that the CNO composition of the nebula is nitrogen enriched ($C/N=0.63$, and $(C+N)/O=0.43$), which is typical of the composition of a metal poor giant atmosphere after CN cycle burning and a first dredge up phase (Schmidt & Nussbaumer 1993). We recall that recently a low metal abundance of the K-star photosphere of $[Fe/H]=-1.3$ was derived (Smith et al. 1996) in agreement with it being a halo object. The UV spectrum in quiescence is the usual in symbiotic systems: a continuum increasing toward the shortest wavelengths with strong narrow emission lines superimposed. The most prominent lines in the quiescence UV spectrum of AG Dra are, in order of decreasing intensity: HeII 1640 Å, CIV 1550 Å, NV 1240 Å, the blend of SiIV and OIV] at 1400 Å, NIV] 1486 Å and OIII] 1663 Å. The continuum becomes flatter longward approximately 2600 Å due to the contribution of the recombination continuum originated in the nebula. Although both continuum and emission lines have been found to be variable during quiescence (e.g. Mikolajewska et al. 1995), there is no clear relation with the orbital period of the system. The ratio intensity of the recombination HeII 1640Å line to the far-UV continuum at 1340 Å suggests a Zanstra temperature of around $1.0-1.1 \times 10^5$ K during quiescence (see Fig. 3).

The large X-ray luminosity together with its soft spectrum allows to understand the large flux from HeII, most notably $\lambda 4686$ Å and $\lambda 1640$ Å, at quiescence (which could not be explained in earlier models; see e.g. Kenyon & Webbink 1984) as being due to X-ray ionization.

5.3. X-ray emission during the optical outbursts

5.3.1. Previously proposed models

Three different basic mechanisms have been proposed to explain the drastic intensity changes of symbiotic stars during the outburst events: (1) Thermonuclear runaways on the surface of the hot component (WD) after the accreted envelope has reached a critical mass (Tutukov & Yungelson 1976, Paczynski & Rudak 1980). The characteristic features are considerable changes in effective temperature at constant bolometric luminosity, and the appearance of an A–F supergiant spectrum thought to be produced by the expanding WD shell. (2) Instabilities in an accretion disk after an increase of mass transfer from the companion (Bath & Pringle 1982, Duschl 1986). (3) Ionization changes of the HII region (from density-bounded to radiation-bounded) around the hot component caused by an abrupt change in the

mass loss rate of the companion (Nussbaumer & Vogel 1987, Mikolajewska & Kenyon 1992). In the case of AG Dra, all these three scenarios have problems with some observational facts. The thermonuclear runaway is rejected by the fact that the quiescent luminosity is already at a level which strongly suggests burning before the outbursts. The disk instability scenario predicts substantial variation of the bolometric luminosity during the outbursts, for which no hints are available in AG Dra. The application of ionization changes to AG Dra is questionable because the nebula is apparently not in ionization equilibrium (Leibowitz & Formigginini 1992).

Specifically for AG Dra an additional scenario has been proposed, namely (4) the liberation of mechanical energy in the atmosphere of the companion (Leibowitz and Formigginini 1992).

5.3.2. Expanding and contracting white dwarf

Using our finding of an anticorrelation of the optical and X-ray intensity and the lack of considerable changes in the temperature of the hot component during the 1994/95 outburst of AG Dra, we propose the following rough scenario. (1) The white dwarf is already burning hydrogen stably on its surface before the optical outburst(s). (2) Increased mass transfer, possibly episodic, from the cool companion results in a slow expansion of the white dwarf. (3) The expansion is restricted either due to the finite excess mass accreted or by the wind driven mass loss from the expanding photosphere of the accretor. This wind possibly also suppresses further accretion onto the white dwarf. The photosphere is expected to get cooler with increasing radius. (4) The white dwarf is contracting back to its original state once the accretion rate drops to its pre-outburst level. Since the white dwarf is very sensitive to its boundary conditions, it is not expected to return into a steady state immediately (Paczynski & Rudak 1980). Instead, it might oscillate around the equilibrium state giving rise to secondary or even a sequence of smaller outbursts following the first one.

The scenario of an expanding white dwarf photosphere due to the increase in mass of the hydrogen-rich envelope has been proposed already by Sugimoto et al. (1979) on theoretical grounds without application to a specific source class. The expansion velocity was shown to be rather low (Fujimoto 1982)

$$\begin{aligned} \frac{dR}{dt} &= R \frac{d \ln R}{d \ln \Delta M_1} \left(\frac{\dot{M} - \dot{M}_{RG}}{\Delta M_1} \right) \\ &\approx 8 \left(\frac{\dot{M} - \dot{M}_{RG}}{10^{-6} M_{\odot} yr^{-1}} \right) \left(\frac{\Delta M_1}{10^{-5} M_{\odot}} \right)^{-1} m.s^{-1} \end{aligned}$$

where $d \ln R / d \ln \Delta M_1 \approx 3 - 4$ at $R \approx 1 R_{\odot}$ was adopted, appropriate for a low mass white dwarf accreting at high rates (Fujimoto 1982). We note in passing that this value could be different at smaller radii, i.e. near white dwarf dimensions (see e.g. Neo et al. (1977)). In particular, depending on the location in the H-R diagram it would be around 2.3 on the high-luminosity plateau of a $0.6 M_{\odot}$ white dwarf, but rising up to 7 around the

high-temperature knee (Blöcker 1996), thus suggesting a non-linear expansion rate. If we assume that the luminosity remains constant during the expansion we can determine the expansion velocity simply by folding the corresponding temperature decrease by the response of the ROSAT detector. Fitting the countrate decrease of a factor of 3.5 within 23 days (from 0.14 cts/s on HJD 9929 to 0.04 cts/s on HJD 9952 corresponding to a concordant temperature decrease from 12.3 eV to 11.1 eV) we find that

$$\left(\frac{\dot{M} - \dot{M}_{\text{RG}}}{10^{-6} M_{\odot} \text{yr}^{-1}} \right) \left(\frac{\Delta M_1}{10^{-5} M_{\odot}} \right)^{-1} \approx 0.8$$

for the input parameters (blackbody radius) corresponding to 2.5 kpc (note that the input parameters change with distance). The mass of the envelope ΔM_1 is difficult to assess due to the non-stationarity in the AG Dra system. In thermal equilibrium at our derived mean temperature it should be larger than $\gtrsim 5 \times 10^{-5} M_{\odot}$ for a white dwarf with mass $M < 0.6 M_{\odot}$ in the steady hydrogen-burning regime (Fujimoto 1982, Iben & Tutukov 1989). Inserting this in the above equation implies that the accretion rate necessary to trigger an expansion which is consistent with the X-ray measurements has to be $(8.1/2.5/1.4) \times 10^{-6} M_{\odot}/\text{yr}$ for white dwarf masses of 0.4/0.5/0.6 M_{\odot} . This is a factor of 40–250 larger than the quiescent burning/accretion rate. The corresponding mean expansion rate is $dR/dt \approx 6.5$ m/s. With a duration of the X-ray decline in 1995 of about 100 days (which is consistent with the 1994 rise time in the optical region) we find that during the 1995 outburst (and probably also during the 1994 outburst) the radius of the accretor roughly doubled while the temperature decreased by about 35% (from 14.5 eV to 9.5 eV for the two parameter fit). The countrate decrease modelled with the above parameters is shown as the dotted line in Fig. 3, and the extrapolation to the quiescent countrate level gives an expected onset of the expansion around HJD = 9902.

A completely different and independent estimate of the response time of a white dwarf gives a similar result, thus it seems quite reasonable that a white dwarf can indeed expand and contract on a timescale (see e.g. Kovetz & Prialnik 1994, Kato 1996) which is observed as optical outburst rise and fall time in AG Dra. The contraction timescale can be approximated by the duration of the mass-ejection phase (Livio 1992), similar to the application to the supersoft transient RX J0513.9–6951 (Southwell et al. 1996), where $\tau \approx 51 / \tilde{m} (\tilde{m}^{-2/3} - \tilde{m}^{2/3})^{3/2}$ days with \tilde{m} being the ratio of white dwarf mass to the Chandrasekhar mass (Livio 1992). This relation gives a timescale of the order of 100 days (as observed) for a white dwarf mass of 0.5–0.6 M_{\odot} , consistent with observations of the AG Dra optical outbursts.

Given the substantial accretion rate triggering the optical outbursts (which has to be supplied by the donor), mass loss via a wind from the cool companion seems to be too low to power the outbursts. Depending on the donor state in quiescence (where wind accretion is possible though we prefer Roche lobe filling; see paragraph 5.1.3.), two possibilities are conceivable: Either the companion fills its Roche lobe all the time, and the outbursts (i.e. the increased mass transfer) are triggered by fluctuations of the cool companion (e.g. radius), or a more massive and/or more

luminous companion produces a strong enough wind to sustain the burning in the quiescent state without filling its Roche lobe and only occasionally overfills its Roche lobe thus triggering the outbursts. As noted above, a Roche lobe filling giant implies a distance larger than the adopted 2.5 kpc. While this imposes no problems with the interpretation of our UV and X-ray data (in fact a larger distance implies a larger intrinsic luminosity and thus shifts AG Dra even further into the stability burning region for even higher white dwarf masses), the distance dependent numbers derived here have to be adapted accordingly.

5.3.3. Wind from the accretor

If the accretion indeed is spherical (i.e. as wind from the donor), it may occasionally be suppressed by the wind from the accretor (Inaguchi et al. 1986). Hot stars with radiative envelopes are thought to suffer intense (radiation-driven) stellar winds at a rate of $\dot{M}_{\text{windloss}} = L/(v_{\text{esc}} c)$ where L is the burning luminosity, v_{esc} is the escape velocity and c the speed of light. This wind becomes increasingly effective at larger radii. Thus, a radiatively driven wind from the WD (Prialnik, Shara & Shaviv 1978, Kato 1983a,b) might restrict the expansion of a RG-like envelope or an expelled shell or even might remove the envelope (Yungelson et al. 1995). An optically thick wind can be even more powerful by up to a factor of 10 (Kato and Hachisu 1994).

The wind of the hot white dwarf has typical velocities of a few hundreds km/s (Kato & Hachisu 1994). At these velocities it would take only several days until this white dwarf wind reaches the Roche lobe of the cool component, i.e. the wind of the cool component. This timescale is short enough to possibly cause the variations in the intensity of those lines which are thought to arise at the illuminated side of the wind zone of the cool component.

5.3.4. Alternative scenario

An alternative to increased mass transfer would be to invoke a mild He flash on the hydrogen burning white dwarf which again might cause the photosphere to expand. Previous investigations for mild flashes have yielded timescales of the order of 15–20 yrs even for the most massive white dwarfs (Paczynski 1975). Recent calculations of H and He flashes have shown that under certain circumstances flash ignition can be rather mild without leading to drastic explosive phenomena, and shorter than about 1 yr already for white dwarf masses below 1 M_{\odot} (Kato 1996).

5.4. UV emission during the optical outbursts

There is an evident mismatch between the outburst UV spectra and the extrapolation toward shorter wavelengths of the blackbodies with temperatures inferred from the ROSAT data (Fig. 5). The most plausible explanation is the existence of an additional emission mechanism in the UV, namely recombination continuum in the nebula surrounding the hot star. While during the quiescent phase the contribution of the nebular continuum is not very large (although it is not negligible), it increases substantially during the outburst. As an example, the change in the

strength of the Balmer jump from July 1994 to December 1995 can be seen in Fig. 4 of Viotti et al. (1996).

5.5. Comparison with other supersoft X-ray sources

Supersoft X-ray sources (SSS) are characterized by very soft X-ray radiation of high luminosity. The *ROSAT* spectra are well described by blackbody emission at a temperature of about $kT \approx 25\text{--}40$ eV and a luminosity close to the Eddington limit (Greiner et al. 1991, Heise et al. 1994). After the discovery of supersoft X-ray sources with *Einstein* observations, the *ROSAT* satellite has discovered more than a dozen new SSS. Most of these have been observed in nearby galaxies (see Greiner (1996) for a recent compilation). Among the optically identified objects there are several different types of objects: close binaries like the prototype CAL 83 (Long et al. 1981), novae, planetary nebulae, and symbiotic systems.

In addition to AG Dra, two other X-ray luminous symbiotic systems with supersoft X-ray spectra are known (RR Tel, SMC 3), both being symbiotic novae. RR Tel was shown to exhibit a similar soft X-ray spectrum (Jordan et al. 1994) and luminosity (Mürset & Nussbaumer 1994). RR Tel is one of the only seven known symbiotic nova systems. It went into outburst in 1945 with a brightness increase of 7^m , and since then declined only slowly. SMC 3 (= RX J0048.4–7332) in the Small Magellanic Cloud was found to be supersoft in X-rays by Kahabka et al. (1994), and has been observed to be in optical outburst in 1981 (Morgan 1992). Simultaneous fitting of the *ROSAT* and UV data was possible only after inclusion of a wind mass loss from the hot component, and gives a temperature above 260 000 K (Jordan et al. 1996). Symbiotic novae are generally believed to be due to a thermonuclear outburst after the compact object has accreted enough material from the (wind of the) companion or an accretion disk.

The similarity in the quiescent X-ray properties of AG Dra to those of the symbiotic novae RR Tel and SMC 3 might support the speculation that AG Dra is a symbiotic nova in the post-outburst stage for which the turn-on is not documented. We have checked some early records such as the Bonner Durchmusterung, but always find AG Dra at the $10\text{--}11^m$ intensity level. Thus, if AG Dra should be a symbiotic nova, its hypothetical turn on would have occurred before 1855. We note, however, that there are a number of observational differences between AG Dra and RR Tel which would be difficult to understand if AG Dra were a symbiotic nova.

If AG Dra is not a symbiotic nova, it would be the first wide-binary supersoft source (as opposed to the classical close-binary supersoft sources) the existence of which has been predicted recently (Di Stefano et al. 1997). These systems are believed to have donor companions more massive than the accreting white dwarf which makes the mass transfer unstable on a thermal timescale.

6. Summary

The major results and conclusions of the present paper can be summarised as follows:

- The X-ray spectrum in quiescence is very soft, with a blackbody temperature of about 14.5 ± 1 eV.
- The quiescent bolometric luminosity of the hot component in the AG Dra binary system is $(9.5 \pm 1.5) \times 10^{36} (D/2.5 \text{ kpc})^2$ erg/s, thus suggesting stable surface hydrogen burning in quiescence. Adopting a distance of AG Dra of 2.5 kpc, the X-ray luminosity suggests a low-mass white dwarf ($M < 0.6 M_{\odot}$).
- In order to sustain the high luminosity the cool companion in AG Dra either has to have a wind mass loss substantially larger than usual K giants or is required to fill its Roche lobe, and consequently has to be brighter than a usual K giant. The mass of the cool component should be smaller than $\approx 2 M_{\odot}$ for the given orbital parameters and the mass ratio would be 2–5.
- The monitoring of AG Dra at X-rays and UV wavelengths did not yield any hints for the predicted eclipse during the times of the U light minima.
- The recent optical outbursts of AG Dra have given us the rare opportunity to study the rapid evolution of the X-ray and UV emission with time. During the optical outburst in 1994 the UV continuum increased by a factor of 10, the UV line intensity by a factor of 2 (see Fig. 2), and the X-ray intensity dropped by at least a factor of 100 (see Fig. 3). There is no substantial time lag between the variations in the different energy bands compared to the optical variations.
- There is no hint for an increase of the absorbing column during the one *ROSAT* PSPC X-ray observation (with spectral resolution) performed during the decline phase of the 1994 optical outburst. Instead, a temperature decrease is consistent with the X-ray data which is also supported by the *IUE* spectral results.
- Modelling the X-ray intensity drop by a slowly expanding white dwarf with concordant cooling, we find that the accretion rate has to rise only slightly above \dot{M}_{RG} . Accordingly, the white dwarf expands to approximately its double size within the about three months rise of the optical outburst. The cooling during this expansion is moderate: the temperature decreases by only about 35%.
- The UV continuum emission during quiescence consists of two components which both match perfectly to the neighbouring wavelength regions (see Fig. 5). Shortwards of $\approx 2000 \text{ \AA}$ it corresponds to the tail of the 14–15 eV hot component as derived from the X-ray observations. However, during the optical outbursts the UV continuum shortwards of $\approx 2000 \text{ \AA}$ does not correspond to the tail of the cooling hot component (9–11 eV), but instead is completely dominated by another emission mechanism, possibly a recombination continuum in the wind zone around the hot component.
- AG Dra could either be a symbiotic nova for which the turn on would have occurred before 1855, or the first example of the wide-binary supersoft source class.

Acknowledgements. We are grateful to J. Trümper and W. Wamsteker for granting the numerous target of opportunity observations with *ROSAT* and *IUE*. We thank Janet A. Mattei for providing recent AAVSO observations of AG Dra, M. Friedjung for discussions on AG Dra properties and D. Schönberner and T. Blöcker for details on the expansion/contraction rate of small core-mass stars. We also thank the referee J. Mikolajewska for a careful reading of the manuscript and helpful comments. JG is supported by the Deutsche Agentur für Raumfahrtangelegenheiten (DARA) GmbH under contract FKZ 50 OR 9201. RV is partially supported by the Italian Space Agency under contract ASI 94-RS-59 and is grateful to Dr. Willem Wamsteker for hospitality at the IUE Observatory of ESA at Villafranca del Castillo (VILSPA). RES thanks NASA for partial support of this research through grants NAG5-2103 (IUE) and NAG5-2094 (ROSAT) to the University of Denver. The *ROSAT* project is supported by the German Bundesministerium für Bildung, Wissenschaft, Forschung und Technologie (BMBF/DARA) and the Max-Planck-Society.

References

- Anderson C.M., Cassinelli J.P., Sanders W.T., 1981, *ApJ* 247, L127
 Bath G.T., Pringle J.E., 1982, *MNRAS* 201, 345
 Beuermann K., Reinsch K., Barwig H., Burwitz V., de Martino D., Mantel K.-H., Pakull M.W., Robinson E.L., Schwobe A.D., Thomas H.-C., Trümper J., van Teeseling A., Zhang E., 1995, *A&A* 294, L1
 Blöcker T., 1996 (priv. comm.)
 Boyarchuk A.A., 1966, *Astrofizika* 2, 101
 Dickey J.M., Lockman F.J., 1990, *Ann. Rev. Astron. Astrophys.* 28, 215
 Di Stefano R., et al. 1997, *ApJ* (in prep.)
 Dobrzycka D., Kenyon S.J., Milone A.A.E., 1996, *AJ* 111, 414
 Duschl W.J., 1986, *A&A* 163, 56
 Fernández-Castro T., González-Riestra R., Cassatella A., Taylor A.R., Seaquist E.R., 1995, *ApJ* 442, 366
 Formiggini L., Leibowitz E.M., 1990, *A&A* 227, 121
 Friedjung M., 1988, in "The symbiotic phenomenon", eds. J. Mikolajewska et al., *IAU Coll.* 103, *ASSL* 145, p. 199
 Fujimoto M.Y., 1982, *ApJ* 257, 767
 Garcia M.R., 1986, *AJ* 91, 1400
 Granslo B.H., Poyner G., Takenaka Y., Schmeer P., 1994, *IAU Circ.* 6009
 Greiner J., Hasinger G., Kahabka P. 1991, *A&A* 246, L17
 Greiner J., 1996, in *Supersoft X-ray Sources*, ed. J. Greiner, *Lecture Notes in Physics* 472, Springer, p. 299
 Greiner J., Schwarz R., Hasinger G., Orio M., 1996, *A&A* 312, 88
 Heise J., van Teeseling A., Kahabka P., 1994, *A&A* 288, L45
 Hric L., Skopal A., Urban Z., Komzik R., Luthardt R., Papoušek J., Hanzl D., Blanco C., Niarchos P., Velic Z., Schweitzer E., 1993, *Contrib. Astron. Obs. Skalnaté Pleso* 23, 73
 Hric L., Skopal A., Chochol D., Komzik R., Urban Z., Papoušek J., Blanco C., Niarchos P., Rovithis-Livaniou H., Rovithis P., Chinarova L.L., Pikhun A.I., Tsvetkova K., Semkov E., Velic Z., Schweitzer E., 1994, *Contrib. Astron. Obs. Skalnaté Pleso* 24, 31
 Huang C.C., Friedjung M., Zhou Z.X., 1994, *A&AS* 106, 413
 Iben I., 1982, *ApJ* 259, 244
 Iben I., Tutukov A.V., 1989, *ApJ* 342, 430
 Iijima T., Vittone A., Chochol D., 1987, *A&A* 178, 203
 Inaguchi T., Matsuda T., Shima E., 1986, *MNRAS* 223, 129
 Jordan S., Mürset U., Werner K., 1994, *A&A* 283, 475
 Jordan S., Schmutz W., Wolff B., Werner K., Mürset U., 1996, *A&A* 312, 897
 Kafatos M., Meyer S.R., Martin I., 1993, *ApJS* 84, 201
 Kahabka P., Pietsch W., Hasinger G., 1994, *A&A* 288, 538
 Kaler J.B., 1987, *AJ* 94, 437
 Kato M., 1983a, *PASJ* 35, 33
 Kato M., 1983b, *PASJ* 35, 507
 Kato M., 1996, in *Supersoft X-ray Sources*, ed. J. Greiner, *Lecture Notes in Physics* 472, Springer, p. 15
 Kato M., Hachisu I., 1994, *ApJ* 437, 802
 Kenyon S.J., 1986, *The symbiotic stars*, Cambridge Univ. Press
 Kenyon S.J., 1988, in "The symbiotic phenomenon", eds. J. Mikolajewska et al., *IAU Coll.* 103, *ASSL* 145, p. 11
 Kenyon S.J., Webbink R.F., 1984, *ApJ* 279, 252
 Kenyon S.J., Garcia M.R., 1986, *AJ* 91, 125
 Kovetz A., Prialnik D., 1994, *ApJ* 424, 319
 Kwok S., Leahy D.A., 1984, *ApJ* 283, 675
 Leibowitz E.M., Formiggini L., 1992, *A&A* 265, 605
 Livio M. 1988, in "The symbiotic phenomenon", eds. J. Mikolajewska et al., *IAU Coll.* 103, *ASSL* 145, p. 149
 Long K.S., Helfand D.J., Grabelsky D.A., 1981, *ApJ* 248, 925
 Luthardt R., 1983, *Mitt. Veränd. Sterne* 9.3, p. 129
 Luthardt R., 1985, *IBVS* 2789
 Luthardt R., 1990, *Contr. of the Astr. Obs. Skalnaté Pleso, CSFR*, vol. 20, p. 129
 Lutz J.H., Lutz T.E., Dull J.D., Kolb D.D., 1987, *AJ* 94, 463
 Mattei J.A., 1995 (priv. comm.)
 Meier S.R., Kafatos M., Fahey R.P., Michalitsianos A.G., 1994, *ApJ Suppl.* 94, 183
 Meinunger L., 1979, *IVBS* 1611
 Mikolajewska J., Kenyon S.J., 1992, *MNRAS* 256, 177
 Mikolajewska J., Kenyon S.J., Mikolajewski M., Garcia M.R., Polidan R.S., 1995, *AJ* 109, 1289
 Montagni F., Maesano M., Viotti R., Altamore A., Tomova M., Tomov N., 1996, *IBVS* 4336
 Morgan D.H., 1992, *MNRAS* 258, 639
 Mürset U., Nussbaumer H., Schmid H.M., Vogel M., 1991, *A&A* 248, 458
 Mürset U., Nussbaumer H., 1994, *A&A* 282, 586
 Neo S., Miyaji S., Nomoto K., Sugimoto D., 1977, *PASJ* 29, 249
 Nussbaumer H., Vogel M., 1987, *A&A* 182, 51
 Paczynski B., 1975, *ApJ* 202, 558
 Paczynski B., Rudak B., 1980, *Acta Astron.* 82, 349
 Piro L., 1986 (priv. comm.)
 Piro L., Cassatella A., Spinoglio L., Viotti R., Altamore A., 1985, *IAU Circ.* 4082
 Prialnik D., Shara M.M., Shaviv G., 1978, *A&A* 62, 339
 Reimers D., 1975, *Mem. Soc. R. Sci. Liege* 8, 369
 Robinson L.J., 1969, *Peremennye Zvezdy* 16, 507
 Robinson K., Bode M.F., Skopal A., Ivison R.J., Meaburn J., 1994, *MNRAS* 269, 1
 Rossi C., Viotti R., Muratorio G., Friedjung M., 1996, *A&AS* (to be subm.)
 Schmidt H.M., Nussbaumer H., 1993, *A&A* 268, 159
 Shakura N.I., Sunyaev R.A., 1973, *A&A* 24, 337
 Skopal A., 1994, *IBVS* 4096
 Smith S.E., Bopp B.W., 1981, *MNRAS* 195, 733
 Smith V.V., Cunha K., Jorissen A., Boffin H.M.J., 1996, *A&A* 315, 179
 Southwell K.A., Livio M., Charles P.A., O'Donoghue D., Sutherland W.J., 1996, *ApJ* 470, 1065
 Sugimoto D., Fujimoto M.Y., Nariai K., Nomoto K., 1979, in *White dwarfs and degenerate variable stars*, *IAU Coll.* 53, eds. H.M. van

- Horn and V. Weidemann, Rochester: University of Rochester Press, p. 280
- Tomov N.A., Tomova M.T., 1997, in Workshop on Symbiotic Stars, Poland, July 1996 (in press)
- Trümper J., Hasinger G., Aschenbach B., Bräuninger H., Briel U.G., Burkert W., Fink H., Pfeffermann E., Pietsch W., Predehl P., Schmitt J.H.M.M., Voges W., Zimmermann U., Beuermann K., 1991, *Nat.* 349, 579
- Tutukov A.V., Yungelson L.R., 1976, *Afz* 12, 521
- Viotti R., 1993, in Cataclysmic Variables and Related Objects, eds. M. Hack and C. la Dous, NASA Monograph Series, NASA SP-507, Washington, USA, p. 634 and 674
- Viotti R., Ricciardi O., Ponz D., Giangrande A., Friedjung M., Cassatella A., Baratta G.B., Altamore A., 1983, *A&A* 119, 285
- Viotti R., Altamore A., Baratta G.B., Cassatella A., Friedjung M., 1984, *ApJ* 283, 226
- Viotti R., González-Riestra R., Rossi C., 1994a, *IAU Circ.* 6039
- Viotti R., Mignoli M., Comastri A., Bedalo C., Ferluga S., Rossi C., 1994b, *IAU Circ.* 6044
- Viotti R., Giommi P., Friedjung M., Altamore A., 1995, *Proc. Abano-Padova Conference on Cataclysmic Variables*: eds. A. Bianchini, M. Della Valle, M. Orio, *ASSL* 205, 195
- Viotti R., González-Riestra R., Montagni F., Mattei J., Maesano M., Greiner J., Friedjung M., Altamore A., 1996, in *Supersoft X-ray Sources*, ed. J. Greiner, *Lecture Notes in Physics* 472, Springer, p. 259
- Yungelson L., Livio M., Tutukov A., Kenyon S.J., 1995, *ApJ* 447, 656
- Yungelson L., Livio M., Truran J.W., Tutukov A., Federova A., 1996, *ApJ* 466, 890
- Zimmermann H.U., Becker W., Belloni T., Döbereiner S., Izzo C., Kahabka P., Schwentker O., 1994, *MPE report* 257